-81-318

CONF-810702--4

MASTER

TITLE: THE SECOND-ORDER PARTICLE-IN-CELL (PIC) COMPUTATIONAL METHOD IN THE ONE-DIMENSIONAL VARIABLE EULERIAN MESH SYSTEM

AUTHOR(S): J. J. Pyun

SUBMITTED TO: Conference on Numerical Methods in Laminar and Turbulent Flows, Venice, Italy, July 1981

DISCLAIMER

[illegible]

By acceptance of this article, the publisher recognizes that the U.S. Government retains a nonexclusive, royalty-free license to publish or reproduce the published form of this contribution, or to allow others to do so, for U.S. Government purposes.

The Los Alamos Scientific Laboratory requests that the publisher identify this article as work performed under the auspices of the U.S. Department of Energy.

University of California

LOS ALAMOS SCIENTIFIC LABORATORY
Post Office Box 1663 Los Alamos, New Mexico 87545
An Affirmative Action/Equal Opportunity Employer

DISTRIBUTION OF THIS DOCUMENT IS UNLIMITED

Form No. 836 R3
[illegible]

UNITED STATES
DEPARTMENT OF ENERGY
CONTRACT W-7405-ENG. 36

THE SECOND-ORDER PARTICLE-IN-CELL (PIC) COMPUTATIONAL METHOD IN THE ONE-DIMENSIONAL VARIABLE EULERIAN MESH SYSTEM

J. J. Pyun

Theoretical Applications Division
Code Development Group
Los Alamos National Laboratory
Los Alamos, New Mexico USA

As part of an effort to incorporate the variable Eulerian mesh into the second-order PIC computational method, a truncation error analysis was performed to calculate the second-order error terms for the variable Eulerian mesh system. The results show that the maximum mesh size increment/decrement is limited to be $\alpha(\Delta r_i)^2$ where Δr_i is a non-dimensional mesh size of the ith cell, and α is a constant of order one.

The numerical solutions of Burgers' equation by the second-order PIC method in the variable Eulerian mesh system were compared with its exact solution. It was found that the second-order accuracy in the PIC method was maintained under the above condition. Additional problems were analyzed using the second-order PIC methods in both variable and uniform Eulerian mesh systems. The results indicate that the second-order PIC method in the variable Eulerian mesh system can provide substantial computational time saving with no loss in accuracy.

1. INTRODUCTION

The purpose of this paper is (1) to determine the maximum mesh size change in the variable Eulerian mesh system in order to maintain the second-order accuracy in the second-order PIC computational method,[1] and (2) to verify the above result by comparing the numerical solution obtained by the second-order PIC method with the known exact solution.

It is well known that the truncation errors[2] in a finite difference equation increase if the mesh size changes rapidly. For example, consider a simple central difference equation for $\frac{du}{dr}$ at a point of $r_{i-\frac{1}{2}}$ as shown in Fig. 1. Expanding a function u in a Taylor series forward and backward from $r = r_{i-\frac{1}{2}}$ gives:

$$u_i = u\left(r_{i-\frac{1}{2}} + \frac{\Delta r_i}{2}\right) = u_{i-\frac{1}{2}} + \frac{\Delta r_i}{2}\left(\frac{du}{dr}\right)_{i-\frac{1}{2}} + \frac{1}{2}\left(\frac{d^2u}{dr^2}\right)_{i-\frac{1}{2}}\left(\frac{\Delta r_i}{2}\right)^2 + O(\Delta r_i^3) \quad (1)$$

$$u_{i-1} \equiv u(r_{i-\frac{1}{2}} - \frac{\Delta r_{i-1}}{2}) = u_{i-\frac{1}{2}} - (\frac{du}{dr})_{i-\frac{1}{2}} \frac{\Delta r_{i-1}}{2}$$

$$+ \frac{1}{2}(\frac{d^2u}{dr^2})_{i-\frac{1}{2}} (\frac{\Delta r_{i-1}}{2})^2 + O(\Delta r^3_{i-1}) \quad . \tag{2}$$

The expression for $(\frac{du}{dr})_{i-\frac{1}{2}}$ is obtained by substracting Eq. (2) from Eq. (1) and dividing the resulting equation by $(\Delta r_i + \Delta r_{i-1})/2$.

$$\frac{du}{dr}_{i-\frac{1}{2}} = \frac{u_i - u_{i-1}}{0.5(\Delta r_i + \Delta r_{i-1})} + \frac{1}{4}(\frac{d^2u}{dr^2})_{i-\frac{1}{2}} (\Delta r_i - \Delta r_{i-1}) + O(\Delta r^2) \tag{3}$$

where by $O(\Delta r^2)$ we mean the largest of $O[2\Delta r_i^3/(\Delta r_i + \Delta r_{i-1})]$, or $O[2\Delta r^3_{i-1}/(\Delta r_i - \Delta r_{i-1})]$. The finite difference Eq. (3) maintains the second-order accuracy if the value of $(\Delta r_i - \Delta r_{i-1})$ is an order of $\sim(\Delta r_i)^2$. However, the accuracy of Eq. (3) deteriates to first order if the mesh size change is greater or equal to $\sim\Delta r_i$. However, if the mesh size changes very slowly such that the fine mesh is used in the region of great interest and the coarse mesh is employed in the reminaing regions, a marked improvement in the overall computational time saving could be achieved without the expense of increasing the density of the mesh system everywhere.

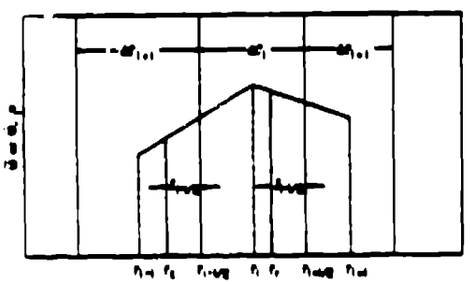

Fig. 1. Change in mesh spacing.

In Section 2 of this paper, the second-order PIC computational method is briefly reviewed. Truncation errors of the second-order PIC computational method are calculated in section 3, and the maximum mesh size change in the variable mesh system is determined based on the second-order truncation error terms in order to maintain the second-order accuracy in the second-order PIC computational method. In section 4 several sample calculations including a simple plane shock and a rarefaction wave are performed, and their numerical solutions by the second-order PIC method are compared with their known exact solutions.

2. REVIEW OF THE SECOND-ORDER PIC COMPUTATIONAL METHOD

Since the detailed descriptions of and applications of the second-order PIC computational method as well as its comparison

with the first-order PIC computations method[7,8] is given in reference 1, only its brief summary will be given here.

Consider a set of one-dimensional (1D) differential equations for compressible fluid flow in a cylindrical geometry. Assuming only one material to be present in a 1D clyinder, a system of equations that we want to solve subject to initial and boundary conditions are:

$$\rho_t + u\rho' = -\rho(u' + \frac{u}{r}) \qquad \text{(mass)} \qquad (4)$$

$$u_t + uu' = -\frac{P'}{\rho} \qquad \text{(momentum)} \qquad (5)$$

$$I_t + uI' = -\frac{P}{\rho}(u' + \frac{u}{r}) \qquad \text{(energy)} \qquad (6)$$

$$P = F(\rho, I) \qquad \text{(equation of state)} \qquad (7)$$

where a subscript, t. denotes a partial derivative with respect to time and the apostrophe means a partial derivative with respective to r hereafter.

In the second-order PIC method the cylinder is divided into a cell of length Δr_i such that a total summation of Δr_i is equal to the radius of the cylinder. The initial velocity U_i, mass M_i and internal energy I_i are assigned to the ith cell such that they represent the initial conditions. Within each cell, the cell mass M_i is divided randomly among a number of "particles" that are distributed throughout the cell so that they approximate the density profile.

The second-order PIC method calculates the quantities at time $(n+1)\Delta t$ in terms of those at time $n\Delta t$ (i.e., an explicit time advancement procedure) where n is a number of timesteps and Δt is a timestep. Within one timestep, the new quantities are computed in two phases:

<u>Phase 1: Lagrangian Phase</u>

(1) Calculate the cell pressure $P^{n+\frac{1}{2}}$ at $(n+\frac{1}{2})\Delta t$ timestep from the equation of state

$$P_i^{n+\frac{1}{2}} = F(\rho_i^{n+\frac{1}{2}}, I_i^{n+\frac{1}{2}}) \quad . \qquad (8)$$

Hereafter, a superscript n denotes a timestep. A subscript i indicates a cell number, and all the variables are cell-centered quantities. Half timestep quantities inside of parenthesis in Eq. (8) are calculated hereafter as below:

$$f_i^{n+\frac{1}{2}} = [f + 0.5\Delta t(f_t + uf')]_i^n \qquad (9)$$

where a quantity f denotes any state variable.

(2) The Lagrangian quantities, $\tilde{u}_i$ and $\tilde{I}_i$, at timestep $(n+1)\Delta t$ are calculated based on $(n+\frac{1}{2})\Delta t$ timestep quantities:

$$\tilde{u}_i = u_i^n - \Delta t\left(\frac{P'}{\rho}\right)_i^{n+\frac{1}{2}} \tag{10}$$

$$\tilde{I}_i = I_i^n - \Delta t\left[\frac{P}{\rho}\left(u' + \frac{u}{r}\right)\right]_i^{n+\frac{1}{2}} \tag{11}$$

(3) Temporarily assign the momentum $M_i\tilde{u}_i$ and total internal energy $M_i\tilde{I}_i$ to cell i.

<u>Phase 2: Particle Transport and Remapping</u>

(1) Move the particles with velocity $\bar{u}(r_r)$ where $\bar{u}(r_r)$ is obtained by linear interpolation of $\bar{u}_i$ $(=0.5\tilde{u}_i^n + 0.5\tilde{u}_i)$ to the particle position r_r. Along with these particles, portions of momentum and internal energy are transported across the cell boundary.

(2) The new total cell mass, momentum, and internal energy are calculated. Subsequently, the new velocity and total specific internal energy are determined.

3. TRUNCATION ERROR ANALYSIS OF THE SECOND-ORDER PIC COMPUTATIONAL METHOD IN THE VARIABLE EULERIAN MESH SYSTEM

Let us consider the velocity and density profiles in Fig. 1 along with a set of 1D differential equations, Eq. (4) through Eq. (7). For convenience, the velocity is assumed to be positive. Let $\ell_{i-\frac{1}{2}}$ and $\ell_{i+\frac{1}{2}}$ be the maximum distances between cell left and right boundaries, and the particle positions from which the particles reach the boundary in timestep Δt as shown in Fig. 1, and the particle velocity leaving a cell (i) is calculated by linear interpolation,

$$\bar{u}(r_r) = [\bar{u} - \ell(\bar{u}_r)]_{i+\frac{1}{2}} \tag{12}$$

where $$\ell_{i+\frac{1}{2}} = \bar{u}(r_r)\,\Delta t \tag{13}$$

$$\bar{u}_{i+\frac{1}{2}} = \frac{\bar{u}_{i+1}\,\Delta r_i + \bar{u}_i\,\Delta r_{i+1}}{\Delta r_i + \Delta r_{i+1}} \tag{14}$$

$$(\bar{u}_r)_{i+\frac{1}{2}} = \frac{\bar{u}_{i+1} - \bar{u}_i}{0.5(\Delta r_{i+1} + \Delta r_i)} \quad . \tag{15}$$

Eliminating $\bar{u}(r_r)$ from Eqs. (12) and (13) gives

$$\ell_{i+\frac{1}{2}} = \frac{\bar{u}_{i+\frac{1}{2}}\,\Delta t}{1 + \Delta t(\bar{u}_r)_{i+\frac{1}{2}}} \quad . \tag{16}$$

Expanding Eq. (16) by using a Taylor series gives:

$$\ell_{i+\frac{1}{2}} = (\bar{u}\Delta t - \bar{u}\bar{u}_r\Delta t^2)_{i+\frac{1}{2}} + O(\Delta t^3) \quad . \tag{17}$$

Here, we neglected the higher than the second-order terms. A similar procedure is used to derive the expression for $\ell_{i-\frac{1}{2}}$

and the result is

$$\ell_{i-\frac{1}{2}} = (\bar{u}\Delta t - \overline{uu_r}\Delta t^2)_{i-\frac{1}{2}} + O(\Delta t^3) \quad . \tag{18}$$

Let $\delta m_{i+\frac{1}{2}}$ be a mass transported from a cell (i) to (i+1), then we have,

$$\delta m_{i+\frac{1}{2}} = 2\pi \int_{r_{i+\frac{1}{2}} - \ell_{i+\frac{1}{2}}}^{r_{i+\frac{1}{2}}} \rho(r) r dr \quad . \tag{19}$$

Assuming that the density, $\rho(r)$, varies linearly, we have

$$\delta m_{i+\frac{1}{2}} = 2\pi[r\rho\ell - (r\rho_r + \rho)\frac{\ell^2}{2} + \frac{1}{3}\rho_r \ell^3]_{i+\frac{1}{2}} \tag{20}$$

$$\text{where } (\rho_r)_{i+\frac{1}{2}} = \frac{\rho_{i+1} - \rho_i}{0.5(\Delta r_{i+1} - \Delta r_1)} \quad . \tag{21}$$

Let $\delta m_{i-\frac{1}{2}}$ be a mass transported from a cell (i-1) to (i), then we could calculate $\delta m_{i-\frac{1}{2}}$ simularily

$$\delta m_{i-\frac{1}{2}} = 2\pi[r\rho\ell - (r\rho_r + \rho)\frac{\ell^2}{2} + \frac{1}{3}\rho_r \ell^3]_{i-\frac{1}{2}} \quad . \tag{22}$$

Then, the net change of a mass in a cell (i), ΔM_i, is calculated as,

$$\Delta M_i = \delta m_{i-\frac{1}{2}} - \delta m_{i+\frac{1}{2}} \quad . \tag{23}$$

Now the density change in cell (i) can be calculated as below

$$\Delta\rho_i = \rho_i^{n+1} - \rho_i^n = \frac{\Delta M_i}{2\pi r_i \Delta r_i} \quad . \tag{24}$$

From a Taylor series expansion of $\rho_i(t + \Delta t)$, we have

$$(\rho_t)_i^n = \frac{\rho_i^{n+1} - \rho_i^n}{\Delta t} - \frac{\Delta t}{2}(\rho_{tt})_i^n - \frac{\Delta t^2}{6}(\rho_{ttt})_i^n + O(\Delta^3) \quad . \tag{25}$$

Here, we truncated the higher than second-order terms. Inserting Eq. (24) into Eq. (25) and, after complex algebraic manipulation, we have

$$\begin{aligned}(\rho_t)_i^n = - [&(\rho u)' + \frac{\rho u}{r} + \Delta t^2 A_1(r,t) + \Delta r_i^2 A_2(r,t) \\ &+ (\frac{\Delta r_{i+1} - \Delta r_i}{\Delta r_i})\Delta t A_3(r,t) - (\frac{\Delta r_i - \Delta r_{i-1}}{\Delta r_i})\Delta t A_3(r,t) \\ &+ \frac{(\Delta r_i^2 + \Delta r_i \Delta r_{i+1} + \Delta r_{i+1}^2)}{\Delta r_i}\Delta t A_4(r,t) \\ &- \frac{(\Delta r_i^2 + \Delta r_i \Delta r_{i-1} + \Delta r_{i-1}^2)}{\Delta r_i}\Delta t A_4(r,t) + O(\Delta^3)]_i^n \quad .\end{aligned} \tag{26}$$

Here, we again truncated the terms higher than the second-order terms. For simplicity, the detailed expressions for the coefficients A_1 through A_4 are not given. However, they are given in reference 9.

Next consider the momentum equation. Let $\delta(m\tilde{u})_{i+\frac{1}{2}}$ be a momentum transported along with particles from a cell (i) to (i+1), then we have

$$\delta(m\tilde{u})_{i+\frac{1}{2}} = 2\pi\int_{r_{i+\frac{1}{2}} - \ell_{i+\frac{1}{2}}}^{r_{i+\frac{1}{2}}} \rho\tilde{u}r\,dr \quad . \tag{27}$$

Again, assuming that the density, $\rho(r)$, and velocity, $\tilde{u}(r)$, vary linearly, we have,

$$\delta(m\tilde{u})_{i+\frac{1}{2}} = \delta m_{i+\frac{1}{2}}(\tilde{u} - \frac{\Delta t}{2}|\tilde{u}|\tilde{u}_r)_{i+\frac{1}{2}} \quad . \tag{28}$$

Let $\delta(m\tilde{u})_{i-\frac{1}{2}}$ be a momentum transported from a cell (i-1) to (i), then we could calculate $\delta(m\tilde{u})_{i-\frac{1}{2}}$ in a similar way

$$\delta(m\tilde{u})_{i-\frac{1}{2}} = \delta m_{i-\frac{1}{2}}(\tilde{u} - \frac{\Delta t}{2}|\tilde{u}|\tilde{u}_r)_{i-\frac{1}{2}} \quad . \tag{29}$$

The net change of a momentum in a cell (i), $\Delta(M\tilde{u})_i$, is calculated as

$$\Delta(M\tilde{u})_i = \delta(m\tilde{u})_{i-\frac{1}{2}} - \delta(m\tilde{u})_{i+\frac{1}{2}} \quad . \tag{30}$$

Now the velocity at timstep $(n+1)\Delta t$ can be calculated in terms of a net momentum change,

$$u_i^{n+1} = \frac{M_i\tilde{u}_i + \Delta(M\tilde{u})_i}{M_i + \Delta(M)_i} = \frac{u_i + \Delta(M\tilde{u})_i/M_i}{1 + \Delta(M)_i/M_i} \quad . \tag{31}$$

Expanding Eq. (31) in terms of a Taylor series results in

$$u_i^{n+1} = [u_i + \frac{\Delta(M\tilde{u})_i}{M_i}](1 - \varepsilon + \varepsilon^2 - \varepsilon^3) + O(\Delta^4) \tag{32}$$

where $\varepsilon = \Delta(M)_i/M_i$.

The truncation error terms higher than the third-order terms are neglected. From a Taylor series expansion of $u_i(t + \Delta t)$, we have

$$(u_t)_i^n = \frac{u_i^{n+1} - u_i^n}{\Delta t} - \frac{\Delta t}{2}(u_{tt})_i^n - \frac{\Delta t^2}{6}(u_{ttt})_i^n + O(\Delta^3) \quad . \tag{33}$$

Here, the truncation error terms higher than the second-order terms are neglected. Inserting Eq. (32) into Eq. (33) and, after complex algebraic manupulation, we have

$$
\begin{aligned}
(u_t)_i^n = [&-uu' - \frac{P'}{\rho} + \Delta t^2 B_1(r,t) + \Delta r_i^2 B_2(r,t) \\
&+ \left(\frac{\Delta r_{i+1} - \Delta r_i}{\Delta r_i}\right)\Delta t B_3(r,t) - \left(\frac{\Delta r_i - r_{i-1}}{\Delta r_i}\right)\Delta t B_3(r,t) \\
&+ \frac{(\Delta r_i^2 + \Delta r_i \Delta r_{i+1}^2 + \Delta r_{i+1}^2)}{\Delta r_i}\Delta t B_4(r,t) \\
&- \frac{(\Delta r_i^2 + \Delta r_i \Delta r_{i-1} + \Delta r_{i-1}^2)}{\Delta r_i}\Delta t B_4(r,t) + O(\Delta^3)_i^n \quad . \qquad (34)
\end{aligned}
$$

Again, the truncation error terms higher than the second-order terms are neglected here. Again, the detailed expressions for the coefficients B_1 through B_4 are not given. However, they are given in reference 9.

A similar algebraic manipulation could be performed for the energy equation, beginning with Eq. (30) and replacing $\tilde{u}_i$ with $\tilde{I}_i$ and the results are

$$
\begin{aligned}
(I_t)_i^n = [&-uI' - \frac{P}{\rho}\left(u' + \frac{u}{r}\right) + \Delta t^2 D_1(r,t) + \Delta r_i^2 D_2(r,t) \\
&+ \frac{(\Delta r_{i+1} - \Delta r_i)}{\Delta r_i}\Delta t D_3(r,t) - \frac{(\Delta r_i - \Delta r_{i-1})}{\Delta r_i}\Delta t D_3(r,t) \\
&+ \frac{(\Delta r_i^2 + \Delta r_i \Delta r_{i+1} + \Delta r_{i+1}^2)}{\Delta r_i}\Delta t D_4(r,t) \\
&- \frac{(\Delta r_i^2 + \Delta r_i \Delta r_{i-1} + \Delta r_{i-1}^2)}{\Delta r_i}\Delta t D_4(r,t) + O(\Delta^3)]_i^n \quad . \qquad (35)
\end{aligned}
$$

The detailed expressions for the coefficients D_1 through D_4 are given in reference 9.

Equations (26), (34) and (35) show that the first-order error terms are identically cancelled out except those terms containing $\Delta t(\Delta r_{i+1} - \Delta r_i)/\Delta r_i$ and $\Delta t(\Delta r_i - \Delta r_{i-1})/\Delta r_i$. In order to maintain the second-order accuracy for the PIC method in the 1D variable Eulerian mesh system, the maximum mesh size change is limited to be $\alpha(\Delta r_i)^2$ where α is a constant of order one.

4. SAMPLE CALCULATIONS AND CONCLUSIONS

To test the second-order PIC method in the variable Eulerian mesh system, three sample problems were analyzed. The first problem is Burgers' equation and the remaining problems are the plane shock and adiabatic rarefaction wave.

4.1 Burgers' Equation

Consider Burgers' equation[3] with the following initial and boundary conditions:

$$u_t - uu_x = \nu u_{xx} \tag{36}$$

$$u(x,0) = u_o \sin \pi x/\ell \tag{37}$$

$$u(0,t) = u(\ell,t) = 0 \quad . \tag{38}$$

The exact solution for the above equation is known and given in reference 4.

A numerical solution for Burgers' equation was obtained by the second-order PIC method in the variable mesh. A truncation error (i.e., a difference between an exact solution and numerical solution) is calculated. Figure 2 shows a ratio of velocity truncation error for doubling a mesh size. A numerical solution by the second-order PIC method is second-order accurate in time and space. Therefore, the velocity truncation error is quadrupled as the mesh size is doubled as shown in Fig. 2. However, the velocity truncation error is not quadrupled as the timestep is doubled. This is because the truncation error terms are dominated by a space error term ($\sim \Delta x_i^2$) as a result of a convergence criterion, $\nu\Delta t/(\Delta x_i)^2 \leq 0.5$. Since it is difficult to double a mesh size at the edges, the ratio of velocity truncation error was not quadrupled.

4.2 Plane Shock Wave

A plane shock wave was analyzed by using the second-order PIC method in both uniform and variable mesh system. These numerical solutions along with their exact solutions[5] in an ideal gas are shown in Figs. 3 through 6. The shock front was handled using an artifical viscosity[6] and a value of its constant coefficient used is 0.5. Figure 3 shows a spatial profile of density at 14 μs. As shown in Fig. 3, the numerical solutions for a spatial density in both uniform and variable mesh system with α=1 agree very well with their exact solutions. The maximum compression ratio for this shock is 4.0 (i.e., a strong shock in an ideal gas). In addition, a computational time saving as a result of using a variable mesh was approximately 30% without loss in accuracy over a uniform mesh case. This computational time saving is due to a smaller number of meshes used in a variable mesh system.

Figures 4 and 5 compare the numerical solutions for a spatial pressure and internal energy in both uniform and variable mesh system with their exact solutions. The mesh size increment constant, α, used here is again 1.0. Again, these numerical solutions agree very well with their exact solutions.

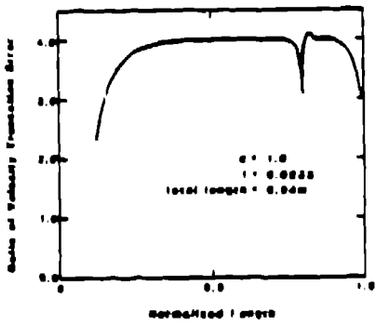

Fig. 2. Ratio of velocity truncation error for doubling mesh size.

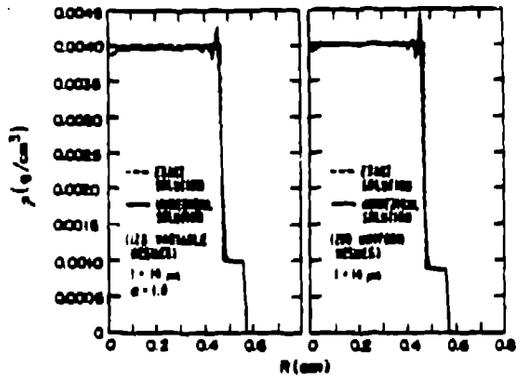

Fig. 3. Density vs R-Distance.

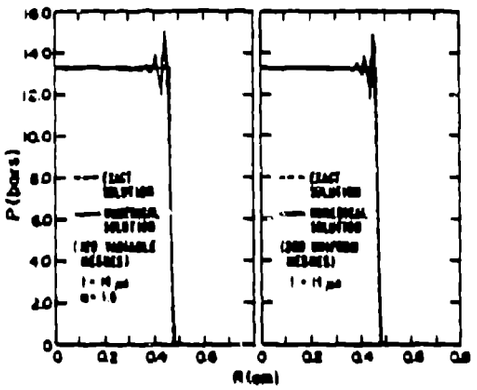

Fig. 4. Pressure vs R-Distance.

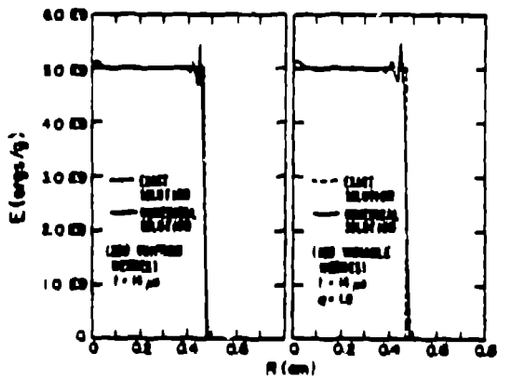

Fig. 5. Internal energy vs R-Distance.

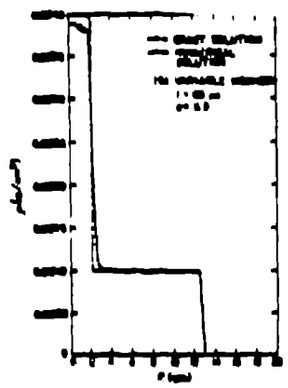

Fig. 6. Density vs R-Distance.

Figure 6 shows a comparison of a spatial density profile at 65 μs for a strong shock in an ideal gas. The variable mesh with incremental constant of 3.3 is used for this numerical solution. The maximum compression ratio if ~ 3.85 for the numerical solution whereas its exact solution is 4.0. This result indicates that the accuracy in the second-order deteriates as the mesh size rapidly increases. As shown in section 3, the maximum mesh size increase in a variable mesh system in order to maintain the second-order accuracy in the second-order PIC method is limited to be $\sim(\Delta r_i)^2$. Here we used the maximum mesh size increase of 3.3 $(\Delta r_i)^2$.

4.3 Plane Adiabatic Rarefaction Wave

A plane adiabatic rarefaction wave was analyzed using the second-order PIC method in both uniform and variable mesh system. These numerical solutions along with their exact solutions[5] in an ideal gas are shown in Figs. 7 through 9. Figures 7 and 8 show a comparison of numerical solutions for a spatial density profile at 15 μs in a uniform and variable mesh system with α=1.0 with their exact solutions. As shown in Figs. 7 and 8 the numerical solutions agree relatively well with their exact solutions. Deviation of numerical solutions from their exact solutions at the edges as shown in Figs. 7 and 8 is due to the vaccum boundary condition. In addition, a computational time saving for this problem was approximately 25% as a result of using a variable mesh over a uniform mesh case.

Figure 9 compares the numerical solution for a spatial density profile at 15 μs in a variable mesh with α=3.3 with its exact solution. The numerical solution at a vaccum boundary deteriates as shown in Fig. 9. However, a computational time saving as a result of using a variable mesh was approximately 50% over a uniform mesh case.

In conclusion, a substantial computational time saving could be achieved in the second-order PIC computational method without sacrifice in accuracy by using a variable mesh system as compared to one using a uniform mesh.

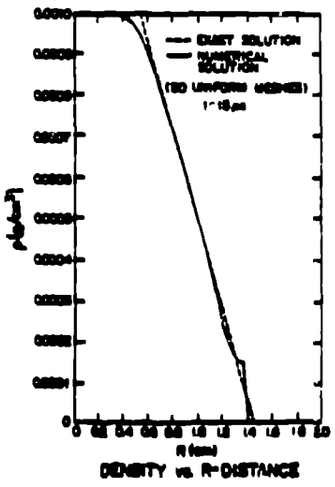

Fig. 7. Density vs R-Distance.

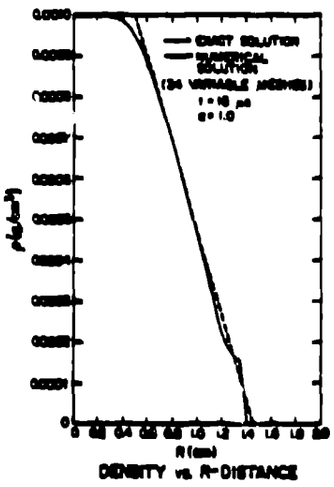

Fig. 8. Density vs R-Distance.

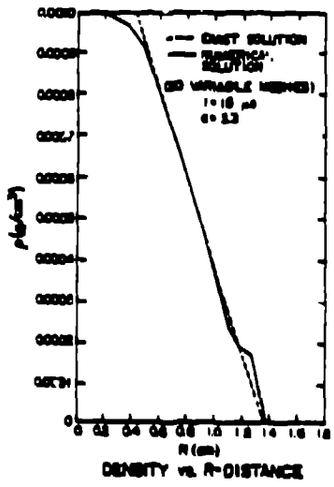

Fig. 9. Density vs R-Distance.

5. REFERENCES

1. Clark, R. A., The Second-Order Particle-In-Cell Computing Method, Accepted for publication in the Journal of Computational Physics, 1980.

2. Crowder, H. J. and Dalton, C., Errors in The Use of Non-Uniform Mesh Systems, J. Computational Physics, Vol. 7, pp.32-45, 1971.

3. Burgers, J., A Mathematical Model Illustrating the Theory of Turbulence, Advances in Applied Mechanics, Vol. 1, pp. 171-199, Academic Press, 1948.

4. Cole, J. D., On a Quasi-Linear Parabolic Equation Occurring in Aerodynamics, Quart. Appl. Math., Vol. 9, pp.225-236, 1951.

5. Harlow, F. H. and Amsden, A. A., Fluid Dynamics, Los Alamos National Laboratory document, LA-4700, 1971.

6. von Neumann, J. and Richtmeyer, R. D., A Method for the Numerical Calculation of Hydrodynamic Shocks, J. Appl. Physics, Vol. 21, pp. 232-237, 1949.

7. Evans, M. W. and Harlow, F. H., The Particle-In-Cell Method for Hydrodynamic Calculations, Los Alamos National Laboratory document, LA-2139, 1957.

8. Amsden, A. A., The Particle-In-Cell Method for the Calculation of the Dynamics of Compressible Fluids, Los Alamos National Laboratory document, LA-3466, 1966.

9. Pyun, J. J., The Second-Order Particle-In-Cell Computational Method in the 2D Variable Eulerian Mesh System, to be published as a Los Alamos National Laboratory document, 1981.

ACKNOWLEDGEMENT

The author is indebted to Dr. Robert A. Clark, Los Alamos National Laboratory, for his encouragement and invaluable guidance throughout the preparation of this paper. The theoretical aspects in particular were made possible through his assistance.